RAPID REPORT

Pathogenic point mutations in a transmembrane domain of the ϵ subunit increase the Ca^{2+} permeability of the human endplate ACh receptor

Amalia Di Castro[1], Katiuscia Martinello[1], Francesca Grassi[1], Fabrizio Eusebi[1,2,3], Andrew G. Engel[4]

[1] *Istituto Pasteur-Fondazione Cenci Bolognetti and Dipartimento di Fisiologia Umana e Farmacologia, Università 'La Sapienza' P.le A. Moro 5; I-00185 Roma, Italy*

[2] *Neuromed, Istituto di Ricovero e Cura a Carattere Scientifico, Via Atinese 18; I-86077 Pozzilli, Italy*

[3] *Istituto di Medicina e Scienza dello Sport, CONI Servizi, Roma, Italy*

[4] *Muscle Research Laboratory, Mayo Clinic, Rochester, MN 55905, USA*

The ϵ subunit of the human endplate ACh receptor (AChR) is a key determinant of the large fraction of the ACh-evoked current carried by Ca^{2+} ions (P_f). Consequently, missense mutations in the ϵ subunit are potential targets for altering the P_f of human AChR. In this paper we investigate the effects of two pathogenic point mutations in the M2 transmembrane segment AChR ϵ subunit, ϵT264P and ϵV259F, that cause slow-channel syndromes (SCS). When expressed in GH4C1 cells, the mutant receptors subunits raise Ca^{2+} permeability of the receptors ∼1.5 and ∼2-fold above that of wild-type, to attain P_f values of 11.8% (ϵT264P) and 15.4% (ϵV259F). The latter value exceeds most P_f values reported to date for ligand-gated ion channels. Consistent with these findings, the biionic Ca^{2+} permeability ratio (P_{Ca}/P_{Cs}) of the mutant AChRs is also increased. Upon repetitive stimulation with ACh, the mutant receptors show an enhanced current run-down compared with wild-type, leading to a strong reduction of their function. We propose that the enhanced Ca^{2+} permeability of the mutant receptors overrides the protective effect of desensitization and, together with the prolonged opening events of the AChR channel, is an important determinant of the excitotoxic endplate damage in the SCS.

(Received 11 January 2007; accepted after revision 31 January 2007; first published online 1 February 2007)
Corresponding author Correspondence: F. Grassi. Dipartimento di Fisiologia Umana e Farmacologia, Università 'La Sapienza' P.le A. Moro 5; I-00185 Roma, Italy. Email: francesca.grassi@uniroma1.it

Slow-channel syndromes (SCS) are caused by point mutations in the human endplate acetylcholine receptor (AChR) that greatly prolong the openings of the AChR channel. In a peculiar form of the SCS, tubulofilamentous inclusions, similar to those found in inclusion body myositis (IBM), accumulate in junctional regions of the muscle fibres (Fidzianska *et al.* 2005). This SCS is caused by a valine-to-phenylalanine substitution at position 259 in the M2 transmembrane segment of the AChR ϵ subunit (ϵV259F) that lines the channel pore.

Hyperphosphorylation of tau protein leads to formation of tubulofilamentous structures in neuronal diseases as well as in IBM, and is associated with, and possibly caused by, a disrupted Ca^{2+} homeostasis (LaFerla, 2002; Pierrot *et al.* 2004). We recently showed that the fractional Ca^{2+} current (P_f) of human endplate AChR, defined as the percentage of the total ACh-evoked current carried by Ca^{2+} ions, is twice as large than that of the homologous mouse AChR (Fucile *et al.* 2006). The high Ca^{2+} permeability of human AChR by itself enhances vulnerability of the human endplate to excitotoxic damage (endplate myopathy) in the SCS. An increased fractional Ca^{2+} current would further contribute to Ca^{2+} overloading of the postsynaptic region and to the Ca^{2+}-dependent pathological effects. Since the human ϵ subunit turned out to be a key determinant of the high P_f at the human endplate (Fucile *et al.* 2006), we postulated that strategically positioned amino acid substitutions in the ϵ subunit can alter the Ca^{2+} permeability of the AChR channel.

To test this notion, we measured the P_f of the ϵV259F-AChR and found it almost twice as high as that of wild-type (WT) AChR. To determine whether this effect is mutation specific, we also examined the P_f for another well-characterized SCS mutation in the M2 segment of the ϵ subunit, ϵT264P (Ohno *et al.* 1995). We found that the P_f of the ϵT264P-AChR is also markedly increased compared

 DOI: 10.1113/jphysiol.2007.127977

with that of the WT receptor. Our results provide the first direct evidence that mutations associated with SCS alter Ca^{2+} permeability as well as channel kinetics of the human endplate AChR.

Methods

Cell cultures and transfection

Rat pituitary GH4C1 cells were grown (5% CO_2, 37°C) in HAM F10 medium plus 10% fetal calf serum and 1% penicillin/streptomycin. Cells were plated onto 35 mm Petri dishes (3×10^5 cells per dish) 24 h prior to transfection. The cDNAs encoding human wild-type α, β, δ, ϵ subunits, or ϵ subunits harbouring the ϵT264P or ϵV259F mutations were transiently transfected using Lipofectamine 2000, using 1 μg of cDNA for each subunit per Petri dish. Medium was changed after overnight incubation with cDNAs, and experiments carried out after a further 24–48 h. All media were purchased from Invitrogen.

Solutions and chemicals

Cells were superfused with a standard external medium containing (mM): 140 NaCl, 2.8 KCl, 2 $CaCl_2$, 2 $MgCl_2$, 10 Hepes-NaOH, 10 glucose, pH 7.3. For cell-attached experiments, patch pipettes were filled with the same solution plus ACh (200 nM).

For whole-cell recordings, patch pipettes were filled with a solution containing (mM): 120 KCl, 5 BAPTA, 10 Hepes-KOH, 2 Mg-ATP, 2 $MgCl_2$, pH 7.3.

For P_f determinations, intracellular solution contained (mM): 140 *N*-methyl-D-glucamine (NMDG), 10 Hepes-HCl, 0.25 Fura-2 pentapotassium salt, 0.001 thapsigargin, pH 7.3. Calibration measurements were performed using an extracellular solution made of (mM): 153 NMDG, 10 $CaCl_2$, 10 Hepes-HCl, pH 7.3.

The shift of the reversal potential of ACh-evoked current was measured using an intracellular solution containing (mM): 140 CsCl, 10 Hepes-CsOH, 20 BAPTA, pH 7.3. The external solution contained (mM): 150 CsCl, 10 Hepes-CsOH, 10 glucose, pH 7.3 plus 1 or 10 $CaCl_2$.

All chemicals were purchased from Sigma (USA), except for Fura-2 pentapotassium salt (Molecular Probes).

Electrophysiology

Currents were recorded using borosilicate glass patch pipettes (2–5 MΩ tip resistance, Sylgard-coated for single-channel recordings) and an Axopatch 200B amplifier (Molecular Devices, Union City, CA, USA). Data were recorded and analysed using pCLAMP 9 (Molecular Devices). All recordings were performed at 25–27°C.

For whole-cell recordings, series resistance was compensated by 80–90%. Cells were voltage clamped at a holding potential of −60 mV and continuously superfused using a gravity-driven fast exchanger perfusion system (RSC-200, BioLogique, France). Current decay and run-down were fitted with single exponential curves [$i(t) = i_\infty + i_0 e^{-t/\tau}$], using Origin 7 (OriginLab Corporation, Northampton, MA, USA).

The relative Ca^{2+} permeability in biionic conditions (P_{Ca}/P_{Cs}) was estimated from the shift of the reversal potential (V_{rev}) of whole-cell ACh-induced current using two different extracellular Ca^{2+} concentrations (Ca_{o1} of 1 mM, Ca_{o10} of 10 mM). In each cell, V_{rev} was calculated at both Ca^{2+} concentrations (V_{r1} and V_{r10}, respectively), by linear interpolation of the ACh-evoked currents peak amplitude plotted *versus* the test potential. The use of voltage ramp yielded inaccurate results because of the rapid desensitization of ϵV259F-AChR. P_{Ca}/P_{Cs} ratios were obtained from the extended Lewis equation adapted to the chosen ion concentrations (Lewis, 1979; Castro & Albuquerque, 1995):

$$\frac{P_{Ca}}{P_{Cs}} = \frac{Cs_o(1 - e^{F\Delta V_r/RT})}{4Ca_{o1}\, e^{F\Delta V_r/RT}\, (1 + e^{FV_{r1}/RT})^{-1} - 4Ca_{o10}(1 + e^{FV_{r10}/RT})^{-1}} \quad (1)$$

where F, R, T are the usual thermodynamic constants and $V_r = V_{r10} - V_{r1}$, Ion activity as given by Castro & Albuquerque (1995), was used in calculations. Membrane potential was stepped to the test potential 1 s before ACh application.

ACh dose–current curves were constructed applying to each cell different doses of transmitter (0.1–300 μM, applied at 30–60 s interval) and normalizing the current response to the plateau value. The data were best-fitted using Hill equation by Origin 7 software (Origin Laboratory).

Single-channel data were filtered at 5 kHz and sampled at 25 kHz. Analysis was performed with a 50% threshold criterion, omitting events shorter than 0.12 ms. Slope conductance was calculated by linear fitting of the unitary amplitudes recorded at different pipette potentials (at least three for each cell). The fit was extrapolated to estimate cell resting potential, which was summed to the pipette potential to obtain membrane potential. The critical time used to identify a burst, determined for each cell from the closed time distribution (Colquhoun & Sakmann, 1985), ranged between 1 and 4 ms.

All results are given as mean ± S.E.M. Two data sets were considered statistically different when $P < 0.05$ (ANOVA test).

Table 1. Single channel properties of WT and mutant AChRs

	WT-AChR	ϵV259F-AChR	ϵT264P-AChR
Conductance (pS)	48.6 ± 2.4 (7)	49.7 ± 1.7 (7)	51.1 ± 2.6 (4)
Burst duration (ms)	1.88 ± 0.19 (5)	47 ± 11 (4)	42.4 ± 7.6 (4)
Critical time (ms)	3.4 ± 0.6 (5)	5 ± 1 (4)	1.8 ± 0.7 (4)
τ_{b1} (ms)/weight (%)	0.59 ± 0.06/49 ± 5 (5)	0.25 ± 0.06/32 ± 3 (4)	0.6 ± 0.2/33 ± 4 (4)
τ_{b2} (ms)/weight (%)	3.2 ± 0.3/51 ± 5 (5)	3.7 ± 2/18 ± 8 (4)	5.6 ± 2.8/17 ± 9 (4)
τ_{b3} (ms)/weight (%)	not present	73 ± 10/50 ± 6 (4)	74 ± 14/50 ± 6 (4)

Data are given as mean ± S.E.M. (number of cells). Burst analysis was performed on cell-attached recordings obtained with bandwidth of 5 kHz; $T = 25$–27°C, with an estimated membrane potential of −90 to −105 mV (as determined *a posteriori* by the *i–V* relation). τ_{b1}, τ_{b2}, τ_{b3}: time constants of the exponential components best fitting the distribution of burst durations.

P_f determination

The methods to measure P_f have been fully reported previously (Fucile *et al.* 2000, 2006). Fluorescence determinations were made using a fluorescence upright microscope (Axioskop 2, Zeiss, Germany), a digital 12-bit cooled camera (SensiCam, PCO, Germany) and a monochromator (Cairn, UK). The system was driven by Axon Imaging Workbench 2 software (Molecular Devices), which also triggered the start of electrophysiological recording. All optical parameters and the setting of the digital camera (50 ms exposure time, 4 × 4 binning) were maintained throughout all measurements. The changes in intracellular calcium were monitored at a single excitation wavelength (380 nm), to achieve a higher time resolution, and expressed as the ratio of time-resolved fluorescence variation over the basal fluorescence ($\Delta F/F_0$).

Only isolated cells with low basal intracellular Ca^{2+} (F_{340}/F_{380} ratio values < 2) were considered for recordings. Cells were filled with Fura-2 pentapotassium salt through the patch pipette and measurements performed after obtaining a stable value of basal fluorescence, with $F_{380} > 200$ arbitrary units (a.u), indicating satisfactory loading. The ratio F/Q (expressed in nC^{-1}) was defined as:

$$\frac{F}{Q} = \frac{\Delta F/F_0}{\int I_{Nic} dt}$$

where I_{Nic} is the nicotine-evoked whole-cell current. The charge entered into the cell was calculated at each fluorescence acquisition time. The F/Q ratio was estimated for each cell as the slope of the linear fit of the *F versus Q* plot. P_f was determined normalizing the F/Q ratio to the calibration value, obtained in a calibration medium containing only Ca^{2+} as permeant ions:

$$P_f = (F/Q_{standard})/(F/Q_{calibration})$$

The $F/Q_{calibration}$ value obtained in this work was $6.6 \pm 1.9\ nC^{-1}$ (mean ± S.E.M., $n = 4$ cells).

Results

Characterization of the ϵV259F and ϵT264P AChRs in GH4C1 cells

We first determined the main functional characteristics of wild-type (WT) and mutant AChRs expressed in GH4C1 cells. We confirmed the slow-channel properties of both ϵV259F- and ϵT264P-AChR at the single-channel level by cell-attached recordings (Fig. 1*A*). For the WT-AChR, the mean single channel slope conductance was about 50 pS and the mean burst duration was 1.9 ms (Table 1). As shown in Fig. 1*B* (left), the distribution of burst duration was fitted by two exponential components, with the mean time constants (τ_{b1} and τ_{b2}) and weights given in Table 1. The duration of the bursts was greatly enhanced by the ϵV259F as well as the ϵT264P mutation, while the conductance of unitary events was not significantly affected (Table 1). The distribution of burst durations presented a third exponential component (time constant, τ_{b3}) for both mutant AChRs. Typical examples are shown in Fig. 1*B* (middle and right panels) and mean values of the τ_bs reported in Table 1. These data confirm that both mutant receptors retain their main functional properties when expressed in GH4C1 cells.

At the macroscopic level, the amplitude of the ACh-evoked currents showed large cell-to-cell variation, ranging from −0.2 nA to over −10 nA at −60 mV (ACh, 100 μM) for each type of AChR, suggesting that expression of the mutant AChRs was not appreciably impaired compared with that of WT-AChR. Both mutant receptors had a higher apparent affinity for ACh, as dose–response curves showed a decrease of the EC_{50} from $33.5 \pm 1.4\ \mu$M ($n = 4$) in the WT-AChR, to $1.2 \pm 0.2\ \mu$M ($n = 4$) and $0.9 \pm 0.2\ \mu$M ($n = 5$) for ϵV259F-AChR and ϵT264P-AChR, respectively (data not shown).

During sustained ACh application, whole-cell currents decayed exponentially, reflecting receptor desensitization. At the plateau concentration of 100 μM, the rate of decay was similar for the WT-AChR ($\tau_{decay} = 207 \pm 28$ ms,

$n = 14$) and the ϵT264P-AChR (246 ± 37 ms, $n = 7$; $P = 0.4$), whereas the ϵV259F-AChR showed a faster decay (128 ± 16 ms, $n = 10$; $P = 0.04$). Repetitive ACh applications produced currents with decreasing peak amplitude (current run-down) for all three AChRs examined (Fig. 1*C*). An exponential fit of the consecutive current peaks showed that WT-AChR (Fig. 1*C*, left) had a relatively slow and limited run-down ($\tau_{\text{run-down}} = 0.78 \pm 0.08$ s, $n = 14$), with an asymptotic amplitude (i_∞) of $31 \pm 4\%$ of the first response. For the ϵV259F mutant (Fig. 1*C*, middle), the decay was both faster ($\tau_{\text{run-down}} = 0.38 \pm 0.06$ s, $n = 9$, $P = 0.002$) and more pronounced ($i_\infty = 4.5 \pm 0.9\%$) than for WT-AChR. The ϵT264P mutant AChR (Fig. 1*C*, right) showed an intermediate behaviour, with a $\tau_{\text{run-down}} = 0.68 \pm 0.05$ s ($n = 7$) and an asymptote at $i_\infty = 9 \pm 2\%$, significantly less than that of WT-AChR ($P = 0.001$). Current run-down was not accompanied by an increased rate of desensitization, as, in each cell, the τ_{decay} of the third current response was not significantly different from that of the first response ($P > 0.5$). Together, these data indicate that the mutant receptors become less responsive than WT, or unresponsive, to ACh at physiological rates of stimulation.

P_f and P_{Ca}/P_{Cs} measurements

For P_f determinations we used nicotine because ACh might activate muscarinic receptors, leading to Ca^{2+} release from internal stores. Currents evoked by nicotine (100 μM) were comparable to those elicited by ACh, except for a slower current decay observed for the WT-AChR ($\tau_{\text{decay}} = 649 \pm 87$ ms, $n = 14$) (e.g. Fig. 2*A*).

Nicotine-evoked Ca^{2+} and current (I_{Nic}) responses were simultaneously recorded (Fig. 2*A*), and the F/Q ratios calculated (Fig. 2*B*). In cells expressing WT-AChR (e.g. Fig. 2*A*, left), normalization to calibration values

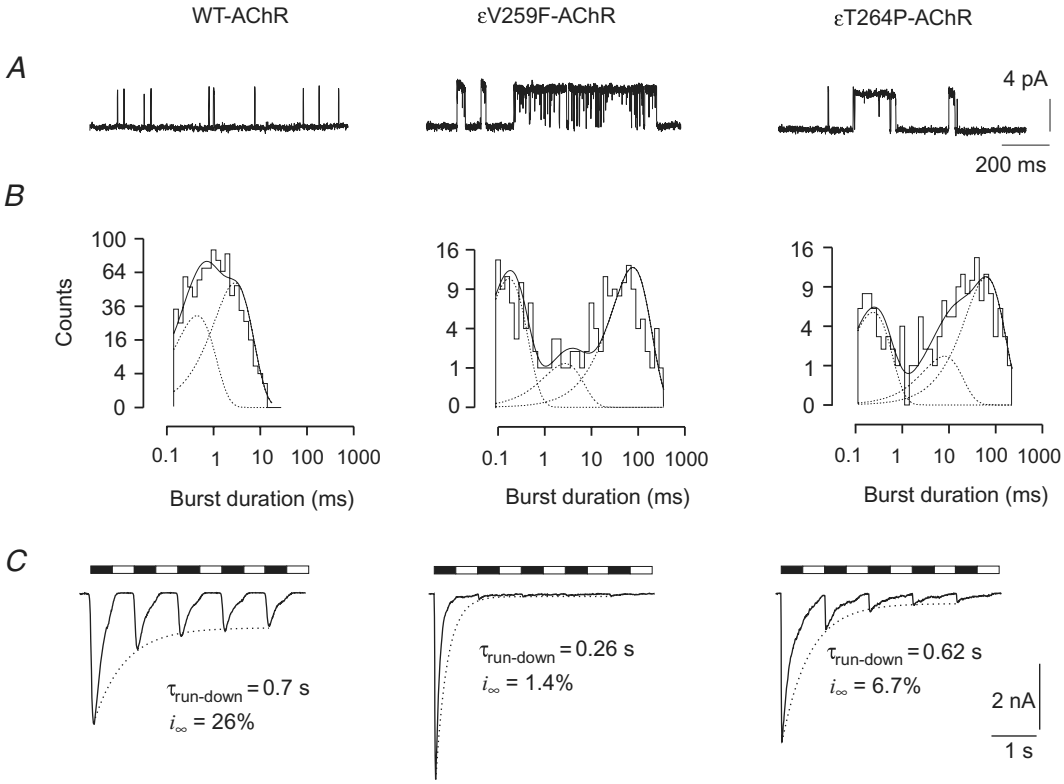

Figure 1. Functional characterization of WT and mutant AChRs in GH4C1 cells
A, typical cell-attached recordings of channel openings evoked by ACh (200 nM) in cells transfected with WT or mutant AChRs, as indicated, revealing prolonged burst duration in ϵV259F and ϵT264P mutant AChRs. Traces were filtered at 1 kHz for display (5 kHz for analysis). Unitary conductance was: 49.8 pS (WT), 46.0 pS (ϵV259F) and 46.6 pS (ϵT264P). *B*, distribution of burst durations for the same recordings as in *A*, best fitted with the sum of two or three exponential components (dotted lines). Time constants (weight) of the fitting distributions in these three cells (at -100 mV membrane potential) were: for WT-AChR, $\tau_{b1} = 0.46$ ms (42%), $\tau_{b2} = 2.9$ ms (58%), critical $\tau = 4$ ms; for ϵV259F, $\tau_{b1} = 0.17$ ms (41%), $\tau_{b2} = 2.7$ ms (14%), $\tau_{b3} = 78$ ms (45%), critical $\tau = 4$ ms; for ϵT264P, $\tau_{b1} = 0.24$ ms (34%), $\tau_{b2} = 7.9$ ms (18%), $\tau_{b3} = 63$ ms (48%), critical $\tau = 1$ ms. *C*, typical whole-cell responses to repetitive ACh (100 μM for 0.5 s) applications (black bars) in cells transfected as indicated. Dotted lines represent the exponential fit of the current peaks with the parameters given on each panel, showing the enhanced run-down of mutant AChRs. Holding potential, -60 mV. Open bars indicate superfusion with standard solution.

yielded P_f values of $7.83 \pm 0.69\%$ ($n = 11$), in excellent agreement with previously published values (Fucile *et al.* 2006). The P_f value measured for ϵV259F-AChR (Fig. 2*A*, middle) was $15.4 \pm 1.7\%$ ($n = 12$, $P = 0.0007$), showing that this mutation doubles the Ca^{2+} permeability of the AChR-channel. For comparison, we measured the P_f of the ϵT264P-AChR (Fig. 2*A*, right) and again found a significantly enhanced Ca^{2+} permeability ($P_f = 11.76 \pm 0.91\%$, $n = 13$, $P = 0.003$). Thus, both slow-channel mutations in the M2 segment of the ϵ subunit enhance the Ca^{2+} permeability of human AChR.

To test by a different approach that the Ca^{2+} permeability of the mutant AChRs was enhanced compared with that of WT-AChR, we also assessed the relative Ca^{2+} permeability of each isoform by measuring its biionic permeability ratio P_{Ca}/P_{Cs}. The currents evoked by ACh (10 μM) were measured at five or more test potentials between -10 and $+10$ mV, bracketing the current reversal potential, at two different extracellular Ca^{2+} concentrations (1 mM and 10 mM) (Fig. 3*A*). With 1 mM extracellular Ca^{2+}, the average values of the reversal potentials were not statistically different for the ϵV259F-AChR (0.2 ± 0.6 mV, $n = 7$) or the ϵT264P-AChR (-0.5 ± 0.3 mV, $n = 10$) *versus* the WT-AChR (0.1 ± 0.3 mV, $n = 8$; $P > 0.2$). The higher extracellular Ca^{2+} concentration induced a right-shift of the reversal potential of each isoform (Fig. 3*B*). Using eqn (1) (see Methods), we obtained $P_{Ca}/P_{Cs} = 0.73 \pm 0.07$ ($n = 7$) for the WT-AChR. The value of P_{Ca}/P_{Cs} obtained for the ϵV259F-AChR (1.20 ± 0.20, $n = 5$) was significantly larger than that of WT-AChR ($P = 0.038$). A further increase over the WT-AChR value was observed in the P_{Ca}/P_{Cs} ratio determined for the ϵT264P-AChR (1.35 ± 0.10, $n = 7$, $P = 0.0007$).

Discussion

This paper provides the first quantitative evidence that the Ca^{2+} permeability of the human endplate AChR can be modified by point mutations in the membrane-spanning M2 segment of the ϵ subunit. The mutations examined, ϵV259F and ϵT264P, gave rise to a fractional Ca^{2+} current of $\sim$15% and $\sim$12%, respectively. These P_f values are among the highest known, being equivalent to, or higher than, those reported for the NMDA receptor (up to 11%, Burnashev *et al.* 1995; 13.5%, Jatzke *et al.* 2002), or the homomeric α7-AChR (11.4%, Fucile *et al.* 2003).

The enhanced Ca^{2+} permeability of the ϵ SCS mutants additionally increases the Ca^{2+} ingress into the junctional sarcoplasm that stems from the prolonged duration of the synaptic current and the intrinsically high Ca^{2+} permeability of human AChR and is thus directly relevant to the pathogenesis of the endplate myopathy associated with the observed mutations. An increased permeability to Ca^{2+} may also occur with SCS mutations in other AChR subunits, as an increase of P_{Ca}/P_{Cs} was observed in HEK 293 cells expressing mouse βV299F-AChR, a mutant receptor designed after a recently identified mutation in a SCS patient (Navedo *et al.* 2006). Both ϵV259F and ϵT264P mutations yield a complex effect on receptor function. The affinity of the mutant receptors for ACh is increased by about one order of magnitude, but this increase is accompanied by (or possibly results in) a loss of receptor function upon repetitive stimulation at

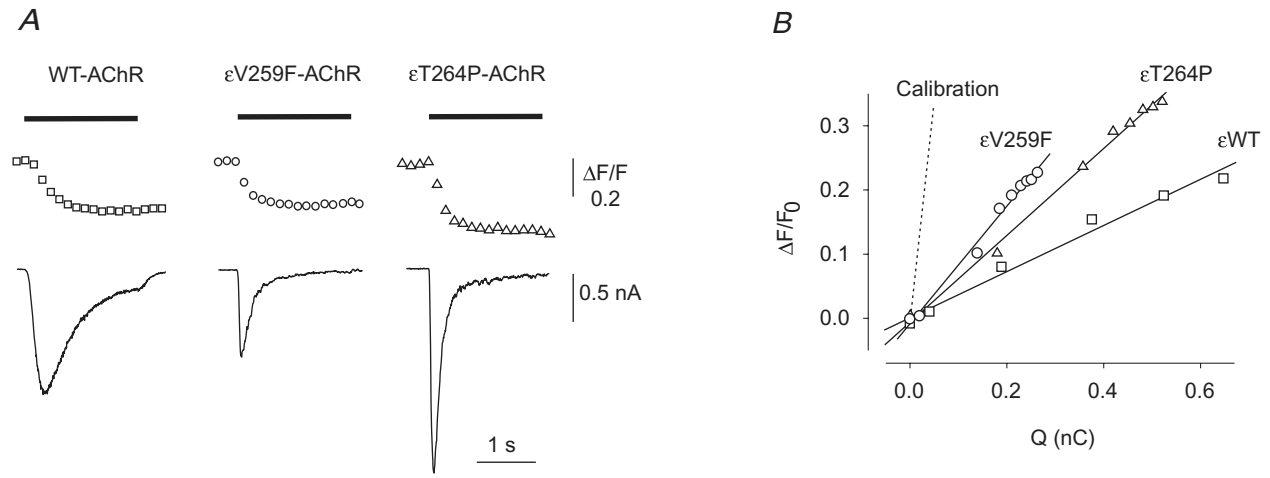

Figure 2. Calcium fractional current of WT and mutant AchRs
A, typical fluorescence (top trace) and current (bottom) responses to nicotine (100 μM, horizontal bar) simultaneously recorded in cells expressing the indicated AChR. Notice the large Ca^{2+} response recorded in the ϵV259 cell in spite of a relatively small current. *B*, linear fit of the $\Delta F/F_0$ *versus* Q in the same three cells as in *A*. The dotted line represents the averaged slope of the calibration experiments. ○, ϵV259F-AChR; △, ϵT264P-AChR; □, WT-AChR, as indicated.

high ACh concentration, as well as an enhanced rate of desensitization in the case of the ϵV259F-AChR. That both mutant AChRs show an increased run-down during repetitive exposure to ACh probably contributes to the abnormal fatigability on exertion observed *in vivo*. Interestingly, the propensity of the mutant receptors to become unresponsive could partially mitigate the adverse effects of the prolonged open time and increased Ca^{2+} permeability of the mutant channels, but not enough to protect the endplate from excitotoxic injury.

In the only patient carrying the ϵV259F mutation identified to date (Fidzianska *et al.* 2005), the endplate myopathy was accompanied by the presence of tubulofilamentous inclusion bodies. The formation of these structures might be precipitated by the severe disruption of Ca^{2+} homeostasis caused by the concurrent prolongation of synaptic events and doubled P_f, consistent with the notion that an altered Ca^{2+} homeostasis enhances phosphorylation of tau protein and formation of fibrillary structures (LaFerla, 2002).

Several lines of evidence indicate that the ϵ subunit is a key determinant of the Ca^{2+} permeability of adult muscle AChR. The P_f is almost 2-fold higher in AChRs containing the ϵ rather than the γ subunit (Villarroel & Sakmann, 1996; Ragozzino *et al.* 1998). Moreover, the ϵ subunit is the only determinant of the high Ca^{2+} permeability of the human adult AChR (Fucile *et al.* 2006). That a valine-to-phenylalanine mutation in the pore-forming M2 segment of the ϵ subunit (ϵV259F) markedly enhances P_f whereas mutation of the corresponding residue in the α subunit (αV249F) has no effect on P_f (Fucile *et al.* 2006), is also consistent with the important role of the ϵ subunit in governing the Ca^{2+} permeability of the human receptor. Another mutation in the ϵ M2 segment, ϵT264P, also increases the P_f of the mutant receptor. Thus, the data presented here confirm that the ϵ subunit has a strong effect on the Ca^{2+} permeability of human endplate AChR.

In our experiments, the alterations in P_{Ca}/P_{Cs} values only partially mirrored those in the P_f. The rapid run-down of current generated by ϵV259F-AChR during multiple applications of ACh limits the accuracy of the P_{Ca}/P_{Cs} measurements. Furthermore, constant field assumptions leading to eqn (1) may not hold under the actual experimental conditions, as previously reported (Vernino *et al.* 1994; Burnashev *et al.* 1995). For instance, studies that compare muscle and neuronal AChRs reveal

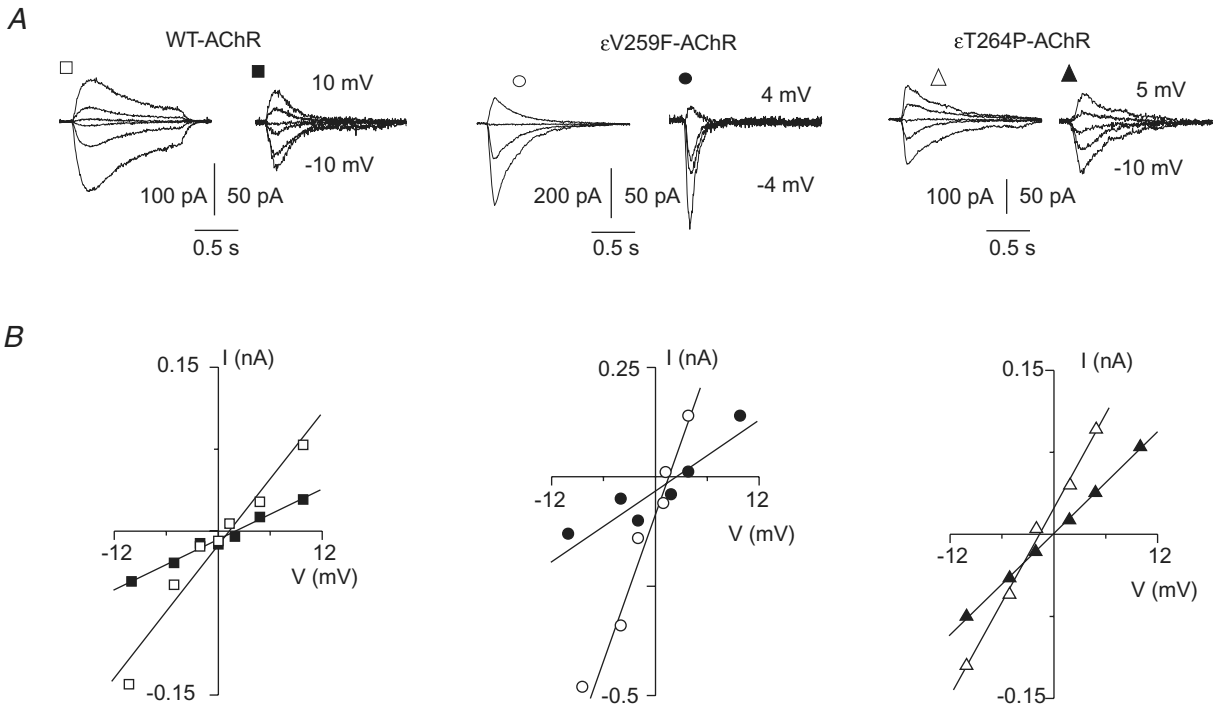

Figure 3. Relative Ca^{2+} permeability (P_{Ca}/P_{Cs}) of WT and mutant AchRs
A, ensemble whole-cell currents recorded in response to ACh (10 μM) applied at various test potentials with low extracellular Ca^{2+} (1 mM, open symbols) or high extracellular Ca^{2+} (10 mM, filled symbols), in transfected cells expressing the indicated AChRs. In each panel, numbers refer to the most positive and negative test potentials shown. Note the reduction of current amplitude in high Ca^{2+} for all the AChR isoforms. *B*, current peak amplitude plotted *versus* membrane test potential in the same cells as in *A*. Lines represent the linear fit of each data group. Note positive shifts of current reversal potentials (0.7 mV for WT-AChR; 1.5 mV for ϵV259F-AChR; 1.6 mV for ϵT264P-AChR) at 10 mM Ca^{2+} (filled symbols).

a 7-fold difference in the P_{Ca}/P_{Cs} ration (Vernino *et al.* 1994), but only a 2-fold difference for the P_f values (Vernino *et al.* 1993). Thus, biionic permeability ratios often provide qualitative rather than quantitative estimates of the relative Ca^{2+} permeability of a given channel whereas P_f determinations require no *a priori* assumptions (Zhou & Neher, 1994) and thus yield a more reliable measure of the Ca^{2+} permeability of the AChR channel (Burnashev *et al.* 1995).

In conclusion, our studies provide further insight into the pathogenic mechanisms whereby single amino acid substitutions in AChR subunits cause disease, which results from the delicate balance between the deleterious effects of the increased Ca^{2+} permeability and the dampening of the synaptic response by run-down of the investigated SCS mutant receptors at physiological rates of stimulation, by loss of AChR from the degenerating folds, and by the altered endplate geometry.

References

Burnashev N, Zhou Z, Neher E & Sakmann B (1995). Fractional calcium currents through recombinant GluR channels of the NMDA, AMPA and kainate receptor subtypes. *J Physiol* **485**, 403–418.

Castro NG & Albuquerque EX (1995). α-Bungarotoxin-sensitive hippocampal nicotinic receptor channel has a high calcium permeability. *Biophys J* **68**, 516–524.

Colquhoun D & Sakmann B (1985). Fast events in single-channel current activated by acetylcholine and its analogues at the frog muscle end-plate. *J Physiol* **369**, 501–557.

Fidzianska A, Ryniewicz B, Shen X-M & Engel AG (2005). IBM-type inclusions in a patient with slow-channel syndrome caused by a mutation in the AChR epsilon subunit. *Neuromuscular Dis* **15**, 753–759.

Fucile S, Palma E, Mileo AM, Miledi R & Eusebi F (2000). Human neuronal threonine-for-leucine-248 α7 mutant nicotinic acetylcholine receptors are highly Ca^{2+} permeable. *Proc Natl Acad Sci U S A* **97**, 3643–3648.

Fucile S, Renzi M, Lax P & Eusebi F (2003). Fractional Ca^{2+} current through human neuronal α7 nicotinic acetylcholine receptors. *Cell Calcium* **34**, 205–209.

Fucile S, Sucapane A, Grassi F, Eusebi F & Engel AG (2006). The human adult subtype ACh receptor has high Ca^{2+} permeability and predisposes to endplate Ca^{2+} overloading. *J Physiol* **573**, 35–43.

Jatzke C, Watanabe J & Wollmuth LP (2002). Voltage and concentration dependence of Ca^{2+} permeability in recombinant glutamate receptor subunits. *J Physiol* **538**, 25–39.

LaFerla FM (2002). Calcium dyshomeostasis and intracellular signaling in Alzheimer's disease. *Nat Rev Neurosci* **3**, 862–872.

Lewis CA (1979). Ion-concentration dependence of the reversal potential and the single channel conductance of ion channels at the frog neuromuscular junction. *J Physiol* **286**, 417–445.

Navedo MF, Lasalde-Dominicci JA, Baez-Pagan CA, Diaz-Perez L, Rojas LV, Maselli RA, Staub J, Schott K, Zayas R & Gomez CM (2006). Novel β subunit mutation causes a slow-channel syndrome by enhancing activation and decreasing the rate of agonist dissociation. *Mol Cell Neurosci* **32**, 82–90.

Ohno K, Hutchinson DO, Milone M, Brengman JM, Bouzat C, Sine SM & Engel AG (1995). Congenital myasthenic syndrome caused by prolonged acetylcholine channel openings due to a mutation in the M2 domain of the epsilon subunit. *Proc Natl Acad Sci U S A* **92**, 758–762.

Pierrot N, Ghisdal P, Caumont AS & Octave JN (2004). Intraneuronal amyloid-β 1-42 production triggered by sustained increase of cytosolic calcium concentration induces neuronal death. *J Neurochem* **88**, 1140–1150.

Ragozzino D, Barabino B, Fucile S & Eusebi F (1998). Ca^{2+} permeability of mouse and chick nicotinic acetylcholine receptors expressed in transiently transfected human cells. *J Physiol* **507**, 749–757.

Vernino S, Amador M, Luetje CW, Patrick J & Dani JA (1992). Calcium modulation and high calcium permeability of neuronal nicotinic acetylcholine receptors. *Neuron* **8**, 127–134.

Vernino S, Rogers M, Radcliffe KA & Dani JA (1994). Quantitative measurements of calcium flux through muscle and neuronal nicotinic acetylcholine receptors. *J Neurosci* **14**, 5514–5524.

Villarroel A & Sakmann B (1996). Calcium permeability increase of endplate channels in rat muscle during postnatal development. *J Physiol* **496**, 331–338.

Zhou Z & Neher E (1993). Calcium permeability of nicotinic acetylcholine receptor channels in bovine adrenal chromaffin cells. *Pflugers Arch* **425**, 511–517.

Acknowledgements

This work was supported by grants from Ministero Istruzione Universita' e Ricerca to F.E. and F.G.; by a grant from Ministero della Salute (Doping 2005) to F.E. and F.G. and by NIH Grant NS6277 and a Muscular Dystrophy Association Grant to A.G.E. A.DiC. is supported by the PhD programme in Neurophysiology of Universita' La Sapienza.